



# Performance of different density functionals for the calculation of vibrational frequencies with vibrational coupled cluster method in bosonic representation

Lalitha Ravichandran<sup>1</sup> · Subrata Banik<sup>2,3</sup>

Received: 10 August 2017 / Accepted: 28 November 2017 / Published online: 6 December 2017  
© Springer-Verlag GmbH Germany, part of Springer Nature 2017

## Abstract

An accurate description of anharmonic vibrational frequencies of polyatomic molecules is a challenging task. It requires an ab initio method to solve the vibrational Schrödinger equation along with extensive electronic structure calculations to generate the quartic potential energy surface (PES) in mass-weighted normal coordinates. The computation of such quartic PES is very expensive. Even for a medium-size molecule, highly accurate ab initio methods like CCSD, CCSD(T) become formidable. The DFT stands as valuable alternative in this case. In this work, we investigate the performances of several commonly used density functionals, namely, B3LYP, BLYP, B3LYPD, M06, M062x, PBE1PBE, B3P86, LC- $\omega$ PBE, X3LYP, B3PW91, and B97D for the evaluation of anharmonic vibrational frequencies of semi-rigid molecules. The quality of the results is assessed by the comparison with experimental values. To this end, we used a set of 19 molecules of various sizes (4–9 atoms). The vibrational coupled cluster method (VCCM) in bosonic representation is used to solve the vibrational structure problem. The hybrid functionals B3P86, B3LYP, B3PW91, PBE1PBE, and X3LYP found to give more accurate result of the fundamental frequencies than the other functionals. Our results show that the error in the BLYP and B97D calculation is due to the inadequate description of the harmonic force field. For the LC- $\omega$ PBE, M06, and M062x, the anharmonic force constants leads to the error. It is found that the comparative performances of the DFT functionals with VCCM are consistent with the second-order vibrational perturbation theory.

**Keywords** Vibrational coupled cluster method · DFT benchmark · VPT2

---

**Electronic supplementary material** The online version of this article (<https://doi.org/10.1007/s00214-017-2177-9>) contains supplementary material, which is available to authorized users.

---

✉ Subrata Banik  
subratachem@gmail.com

Lalitha Ravichandran  
lalithravi@gmail.com

- <sup>1</sup> School of Chemistry, University of Hyderabad, Hyderabad 500046, India
- <sup>2</sup> Advanced Centre for Research in High Energy Materials, University of Hyderabad, Hyderabad 500046, India
- <sup>3</sup> Manipal Centre for Natural Sciences, Manipal University, Manipal 576104, India

## 1 Introduction

The techniques of vibrational spectroscopy (both IR and Raman) have become essential tools to understand the structure and dynamics of molecules and now widely used in many areas of research [1–3]. A detail understanding of the theory of vibrational motions in a molecule is necessary for the analysis and interpretation of the experimental spectra. The harmonic approximation to the vibrational motion has been proved to be a very efficient approximation to analyze and assign the vibrational spectra of even large molecules. Despite the simplicity of the harmonic oscillator approximation, it often fails to describe several features and give desirable accuracy of the band positions to study the experimental spectra obtained in the modern highly accurate experimental techniques. With the increase in computer performances, and development of several cost-efficient accurate quantum chemical methods, the calculations of vibrational spectra beyond harmonic approximation gained

considerable interest over last few years. However, the accurate description of anharmonic vibrations in polyatomic molecule is a challenging problem. The effects of anharmonicity on the vibrational transitions differ significantly from molecule to molecule. Several representations have been proposed for the vibrational Hamiltonian in different coordinate systems [4–6]. Within the limitations involve in them, each coordinate system has some advantages over the other depending on the nature of vibrations. Among these, the Watson Hamiltonian, represented in the mass-weighted normal coordinates, is the most commonly used Hamiltonian for the vibrational calculation of the semi-rigid polyatomic molecule

$$H = \sum_i \frac{P_i^2}{2} + V(q) + V_W + V_c. \quad (1)$$

Here,  $q_i$  and  $P_i$  are the mass-weighted normal coordinates and their conjugate momenta, respectively.  $V_W$  and  $V_c$  are the Watson mass-dependent term and Coriolis coupling term. The potential energy function  $V(q)$  is usually represented by a quartic polynomial of the Taylor series expansion in the mass-weighted normal coordinates

$$V(q) = \frac{1}{2} \sum_i \omega_i^2 q_i^2 + \sum_{i \leq j \leq k} f_{ijk} q_i q_j q_k + \sum_{i \leq j \leq k \leq l} f_{ijkl} q_i q_j q_k q_l. \quad (2)$$

Here,  $\omega_i$  is the harmonic frequency of  $i$ th vibrational mode. These frequencies are obtained as the eigenvalues of the Hessian matrix in the mass-weighted Cartesian coordinates. The set of eigenvectors of the Hessian matrix defines the normal coordinates.  $f_{ijk}$  and  $f_{ijkl}$  are the third and fourth derivatives of electronic energy with respect to the normal coordinates at the equilibrium geometry of molecule. The computation of these force constants is a major bottleneck in the vibrational calculation. Several algorithms to compute them have been proposed, and they are available in many of the popular quantum Chemistry packages like Gaussian [7], Molpro [8], Gamess [9].

The Watson Hamiltonian with the potential in Eq. 2 is a many-body Hamiltonian, and consequently, the exact analytic solution of the associated Schrödinger equation is not possible. Over the years, several ab initio methods have been developed to solve the Schrödinger equation associated with this Hamiltonian. The vibrational second-order perturbation theory is developed and used widely [10–16]. Here, the harmonic part of the Hamiltonian is taken as the zeroth-order Hamiltonian, and the cubic and quartic terms of the potential are treated as perturbations. Alternatively, the vibrational self-consistent field (VSCF) method is developed based on variation principle and used extensively by many authors [17–21]. Here, the many-body Hamiltonian is approximated as the sum of an effective independent

one body Hamiltonian for each mode. The potential of the single-particle Hamiltonian is generated by averaging the many-body potential over the other modes. Several post-VSCF methods are developed to account the vibrational correlation effects [22–34], that are missing in the VSCF description. Among these correlation methods, the vibrational coupled cluster method (VCCM) [24–40] is found to be one of the most accurate methods to calculate the vibrational spectra. The VCCM has been successfully applied to compute the vibrational transition energies, IR and Raman spectra of polyatomic molecules, and the results are found to be comparable with the experimental results even with a low-order truncation [38, 41, 42].

Given a vibrational structure method, the accuracy of a vibrational calculation and its computational cost depend on the electronic structure method to generate the quartic PES. The use of a highly accurate wave function-based method, e.g., CCSD, CCSD(T), improves the computed frequencies significantly, and the results are found to be close to the experimental values [43]. However, the high computational costs of these methods limit their use to only small- or medium-size molecules. In this respect, the density functional theory provides a valuable alternative. The DFT is much cheaper than the wave function-based methods for electron correlation and thus is widely used in computation especially for the systems of large size where the wave function-based methods are intractable. However, unlike the wave function-based methods, where the systematic improvement is possible by improving the quality of wave function (e.g., by including the higher-order terms in perturbation analysis, or, including the higher excitations), there is no way to improve the DFT results in a systematic manner. The exchange part of the density functional formulation is empirical to a great extent. Due to this empirical foundation, numerous DFT methods have been proposed. The most of the modern developments of the DFT method use experimental data from wide range of chemical systems to enhance the accuracy of calculation. As a consequence, no DFT method gives uniform accuracy for different chemical properties or systems. This motivated several works that illustrated the performance of the DFT methods for different properties [44–50]. There have been several studies to benchmark the performances of the DFT functionals for the anharmonic frequencies [51–55]. However, to the extent of our knowledge, such comparative studies have been limited to the VPT2 method.

The goal of the present work is to make quantitative assessment of different density functionals to generate the quartic PES for the calculation of the anharmonic vibrational frequencies using vibrational coupled cluster method. For this purpose, we investigate the performance of several commonly used density functionals, namely B3LYP, BLYP, M06, M062x, PBE1PBE, B3P86, B97D, LC- $\omega$ , X3LYP,

B3PW91, and B3LYPD, to calculate the frequencies of vibrational fundamental transitions in semi-rigid molecules. The quality of the results is assessed by comparison with experimental values. We used a set of 19 semi-rigid molecules of various sizes (4 atoms–9 atoms). The resultant accuracy in the VCCM description of the anharmonic transition energies with the quartic PES generated by using these functionals is analyzed in terms of the different exchange and correlation functionals used in the formulation of these DFT methods.

Given such a benchmark study on the performance of different functionals to calculate the vibrational transition energies with VCCM calculations, it is important to see whether such assessments of the DFT functionals is specific to only VCCM, or holds in general for other vibrational structure theories. For this purpose, we investigate the performances of the functionals with second-order vibrational perturbation theory (VPT2).

The paper is organized as follows. In the next section, we give brief discussions of the computational details used in this study. In the subsequent section, we discuss the results. Finally, the observations are summarized in Summary section.

## 2 Computational details

### 2.1 PES generation

We used Gaussian09.B01 quantum chemistry software to calculate the quartic PES. It uses analytic Hessian to compute the harmonic frequencies, and the cubic and quartic force constants are evaluated by numerical differentiations of the analytic Hessian around equilibrium geometry. The geometries of the molecules are optimized with ‘opt=tight’ option as recommended by Barone [11]. Recently Martin and co-workers found that the DFT functionals, particularly the meta-GGA Minnesota functionals, need large number of grid points for numerical integrations to compute the quartic PES [16, 54]. We used pruned grid (150,974) for molecules with second row elements and (225,974) for molecules with third row elements. Such large grid leads to convergence of fundamental frequencies within  $1\text{ cm}^{-1}$  in the VPT2 calculations, as pointed by Kesharwani et.al. [54]. We used 6–311++(2d,2p) basis set in all the electronic structure calculations. We anticipate that the errors in the resultant anharmonic frequencies due to the size of the basis set will not be significant.

### 2.2 The DFT methods

The development of the generalized gradient approximation (GGA) [56, 57] for the exchange correlation

functional made the DFT applicable to chemistry with convincing results for molecular geometries and dissociation energies. However, the major breakthrough came with the development of hybrid functional B3LYP [58], where, a portion of the Hartree Fock (HF) exchange term was combined with the GGA exchange functional of Becke (B88) [56] and correlation functional of Lee, Yung and Parr (LYP) [59]. The B3LYP functional became incredibly successful and widely used in numerous calculations. Following the success of B3LYP, many hybrid functionals are proposed and applied extensively for various molecular studies. Later on, many other DFT functionals were developed to overcome the challenges that the conventional hybrid functionals face [60], for example, the accurate calculations of dispersion/van der Waals interactions [60–62], reaction barriers [63, 64], long-range interactions [65], the electronic states with degeneracy or near degeneracy [66]. These formalisms involve the use of various percentage of HF exchange term, different exchange and correlation functionals, kinetic energy-dependent functionals, dispersion correction terms. We used following functionals to generate the quartic PES for the present study.

**BLYP** One of the preliminary GGA functional that is widely used for electronic structure calculation in molecules. It combines B88 exchange functional and LYP correlation functional. The LYP functional has both local and non-local correlation.

**B3LYP** The most used density functional in the literature. This hybrid functional has 20% of ‘exact’ HF exchange correlation term. In the Gaussian implementation, three unknown parameters were obtained by fitting experimental data from G1 data set [67] of Pople and co-workers. The final form of the functional is

$$0.2E_x^{\text{HF}} + 0.8E_x^{\text{Slater}} + 0.72\delta E_x^{\text{B88}} + 0.81E_c^{\text{LYP}} + 0.19E_c^{\text{VWN}}. \quad (3)$$

Here  $E_c^{\text{VWN}}$  is the correlation functional of Vosko, Wilk and Nusair [68], often referred as local density correlation.  $E_c^{\text{LYP}}$  functional contains only the non-local terms of LYP functional.

**B3LYPD** The B3LYP functional with the inclusion of Grimmes dispersion correction (D2 version) [69].

**B3P86** Three parameter hybrid functional like B3LYP, except the non-local term of LYP functional is replaced by the non-local term of Perdew 1986 [70].

**B3PW91** Similar to B3LYP and B3P86. The non-local correction functional is replaced by the non-local part of gradient-corrected Perdew and Wang 1991 correlation functional [71].

**PBE1PBE** This hybrid functional was developed by Adamo and Barone [72] from the pure gradient-corrected functional of Perdew, Burke and Ernzerhof (PBE) [57] with 25% of exact HF exchange and 75% of correlation weighting.

**B97D** This standalone functional includes dispersion correction by Grimme [73] over Becke's 'mapped reduced gradient-dependent auxiliary function' of 1997 [74].

**LC- $\omega$ PBE** Long-range corrected functional form of PBE [75]. It contains 0% HF exchange if inter electronic distance is less than  $\omega$  and 100% HF exchange if the inter electronic distance is more than  $\omega$ . In Gaussian implementation the default value for  $\omega$  is 0.4 bohrs.

**X3LYP** Another hybrid functional (eXtended) [76] with LYP correlation term. Here, the exchange functional is a combination of B88 and PW91. This contains 21.8% HF exchange.

**M06** Minnesota functional of Truhlar and co-workers [77]. The Minnesota functionals are based on the meta-GGA approximation. These functionals include terms that are dependent on the kinetic energy density. The M06 functional contains 27% HF exchange.

**M062x** Another Minnesota functional with 54% HF exchange [77]. It is found to be more accurate than M06 for thermo-chemistry, kinetics, and non-covalent interactions.

### 2.3 Vibrational coupled cluster method in bosonic representation

Over the last decade, extensive works were done for the formulation of vibrational coupled cluster method [28, 29, 32–34, 36, 78, 79]. Two different routes are followed for the VCCM formalism. One is the basis set representation, developed and used by Christiansen and co-workers [28, 29, 78], and the other one is the bosonic representation developed by Prasad and co-workers [32–34, 36, 79]. We used the bosonic representation.

The formulation of the VCCM in bosonic representation follows three steps. In step 1, we invoke an effective harmonic oscillator (EHO) [32, 80] approximation for the vibrational ground-state reference wave function. In the EHO, a product of  $N$  Gaussian functions

$$\Phi_0 = \exp\left(-\sum_{i=1}^N \omega_i (q_i - q_i^0)^2 / 2\right), \quad (4)$$

is variationally optimized with respect to the  $\omega_i$  and  $q_i^0$  to obtain the optimized ground-state function. Here  $N$  is the number of vibrational degree of freedom in the molecule. The harmonic oscillator ladder operators are defined with respect to this EHO wave function

$$a_i = \sqrt{\frac{\omega_i}{2}} \left( q_i - q_i^0 + \frac{1}{\omega_i} \frac{q}{dq_i} \right) \quad (5a)$$

$$a_i^\dagger = \sqrt{\frac{\omega_i}{2}} \left( q_i - q_i^0 - \frac{1}{\omega_i} \frac{q}{dq_i} \right). \quad (5b)$$

The EHO wave function,  $\Phi_0$ , by definition, is the vacuum state for the operator  $a_i$ .

In step 2, the VCCM wave function for the ground state is parametrized with a double-exponential wave operator

$$|\Psi_g\rangle = e^S e^{-\sigma} |\Phi_0\rangle. \quad (6)$$

Here,

$$S = \sum_i s_i a_i^\dagger + \sum_{i \leq j} s_{ij} a_i^\dagger a_j^\dagger + \sum_{i \leq j \leq k} s_{ijk} a_i^\dagger a_j^\dagger a_k^\dagger + \dots \quad (7a)$$

$$\sigma = \sum_i \sigma_i a_i + \sum_{i \leq j} \sigma_{ij} a_i a_j + \sum_{i \leq j \leq k} \sigma_{ijk} a_i a_j a_k + \dots \quad (7b)$$

We invoke the subsystem embedding condition [81, 82] to derive the working equations for  $S$  and  $\sigma$  matrix elements. Under this condition, the equations for the excitation cluster matrix elements  $S$  are decoupled from the equations for the de-excitation cluster matrix elements  $\sigma$ . The final working equations for the cluster matrix elements  $S$ , the ground-state energy and the cluster matrix elements  $\sigma$  are

$$\langle \Phi_e | H_{\text{eff}}^1 | \Phi_0 \rangle = 0, \quad (8)$$

$$\langle \Phi_0 | H_{\text{eff}}^1 | \Phi_0 \rangle = e_g, \quad (9)$$

$$\langle \Phi_0 | H_{\text{eff}}^2 | \Phi_e \rangle = 0. \quad (10)$$

Here,  $\Phi_e$  are excited states. The effective Hamiltonian  $H_{\text{eff}}^1$  and  $H_{\text{eff}}^2$  are defined as

$$H_{\text{eff}}^1 = e^{-S} H e^S, \quad (11a)$$

$$H_{\text{eff}}^2 = e^\sigma e^{-S} H e^S e^{-\sigma} \quad (11b)$$

We used four-body approximation for the cluster operator  $S$  and  $\sigma$  in Eq. 7. Since the Hamiltonian is a four-body operator, the effective Hamiltonian  $H_{\text{eff}}^1$  and  $H_{\text{eff}}^2$  are also approximated to have at most four-body terms.

In the step 3, the coupled cluster linear response theory [83, 84] (CCLRT) is used to calculate the vibrational excitation energies. In this approach, the double similarity transformed effective Hamiltonian,  $H_{\text{eff}}^2$  is diagonalized over the configuration space of excited states of EHO. The diagonalization of  $H_{\text{eff}}^2$  gives the excitation energies directly.

In our earlier studies [41, 42], we noted that in the frequency region dominated by CH stretching fundamentals, the zeroth-order CH fundamental states mix strongly with several higher quanta states due to high-order resonances. Due to such heavy mixing of the zeroth-order states, one may occasionally get more than one final states that carry significantly large contributions from zeroth-order CH fundamental states. In this situation, we choose the state that

has highest contribution from the zeroth-order fundamental as the final fundamental state.

Note that the present calculations exclude the Coriolis coupling terms from the Hamiltonian.

## 2.4 Second-order vibrational perturbation theory

The second-order vibrational perturbation theory (VPT2) [10–15] is the one of the most widely used method to calculate the anharmonic vibrational spectra of polyatomic molecules. In this work, we used Gaussian09.B01 package to calculate the VPT2 anharmonic frequencies. A modified version of VPT2 method is implemented in Gaussian09 by Barone and co-workers [11–13]. In this method, the harmonic part of the vibrational Hamiltonian is taken as the zeroth-order Hamiltonian and the cubic, quartic and Coriolis coupling terms are treated as perturbations. The working equations for the fundamentals are given by

$$E(v) = \chi_0 + \sum_i \omega_i \left( v_i + \frac{1}{2} \right) + \sum_{i < j} \chi_{ij} \left( v_i + \frac{1}{2} \right) \left( v_j + \frac{1}{2} \right). \quad (12)$$

Here,  $\omega_i$  is the harmonic frequency of  $i$ th mode,  $v_i$  are the vibrational states, and  $\chi_0$  and  $\chi_{ij}$  are zero point contribution and anharmonic constants, respectively, derived from cubic, quartic and Coriolis coupling terms of the PES. We note that the computations of the anharmonic constants encounter singularities if there are strong Fermi resonances present between the vibrational modes. To overcome such singularity problem, Barone used variational calculations with the modes involving Fermi resonances [11]. We used the default

threshold values implemented in Gaussian09 to detect the vibrational resonances (10  $\text{cm}^{-1}$  for both Fermi and Darling–Dennison resonances).

## 3 Results and discussions

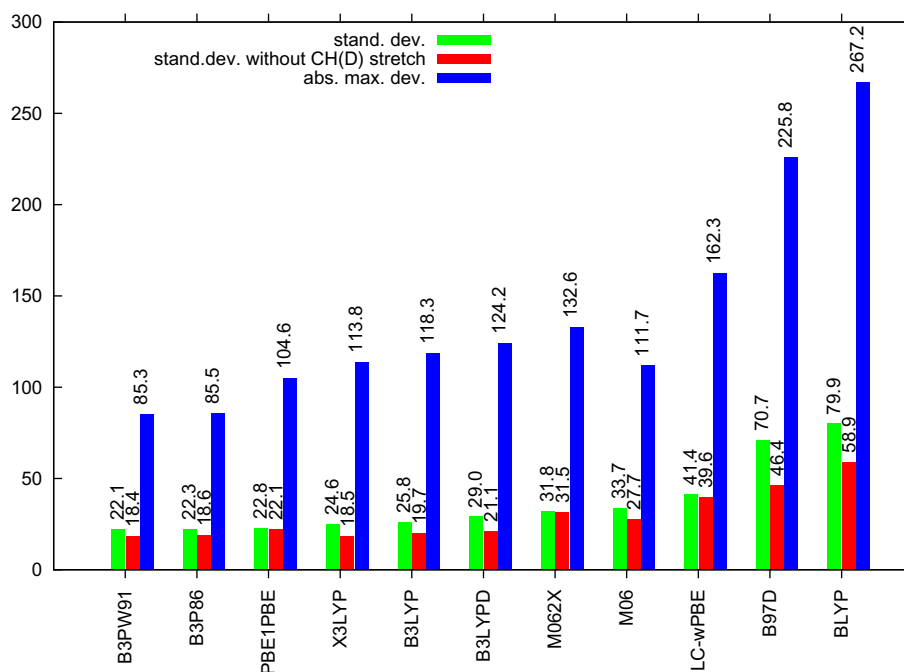
In Fig. 1, we present the accuracy of VCCM anharmonic frequencies for the fundamental transitions with respect to the experimental values in terms of the standard deviation (SD) and the maximum absolute deviation (MaxAD). The standard deviations are calculated using the formula

$$SD = \sqrt{\frac{1}{M-1} \sum_{i=1}^M (v_i^{\text{exp}} - v_i^{\text{anh}})^2} \quad (13)$$

Here,  $v_i^{\text{exp}}$  and  $v_i^{\text{anh}}$  are the experimental and calculated anharmonic frequencies, respectively, and  $M$  is the total number of fundamental transitions considered in the calculations. Except, for  $\text{C}_2\text{H}_4\text{O}$  [85],  $\text{C}_2\text{H}_4\text{O}$  [85] and Furan [86] molecule, all the experimental frequencies are taken from NIST database [87]. The fundamentals with known experimental frequency (a total of 166 transitions) are used to calculate the SD.

The best results are found with the hybrid functionals B3PW91, B3P86, and PBE1PBE. These three hybrid DFT methods have different versions of correlation functional of Perdew and co-workers. The SD values with B3PW91, B3P86, and PBE1PBE are 22.1, 22.3 and 22.8  $\text{cm}^{-1}$ , respectively, and the MaxAD values are about 85, 85, and

**Fig. 1** The standard deviations of errors (in  $\text{cm}^{-1}$ ) in the VCCM calculations





105  $\text{cm}^{-1}$ , respectively. Thus, the most accurate results are found with B3PW91 functional. However, the accuracy with these three functionals are nearly identical.

The B3LYP and X3LYP functionals are found to be less accurate than B3PW91, B3P86, and PBE1PBE functionals. For example, the SD of B3LYP (25.8  $\text{cm}^{-1}$ ) is about 3.7  $\text{cm}^{-1}$  higher than the most accurate method B3PW91. The MaxAD value of B3LYP is about 118, 33  $\text{cm}^{-1}$  higher than MaxAD of B3PW91. Thus, our results suggest that the correlation functions of Perdew and co-workers improve accuracy over the LYP correlation function. We note marginal improvement of accuracy with X3LYP functional over the B3LYP. The SD of X3LYP (24.6  $\text{cm}^{-1}$ ) is about 1.2  $\text{cm}^{-1}$  less than SD of B3LYP. The MaxAD value of X3LYP (114  $\text{cm}^{-1}$ ) is only 4  $\text{cm}^{-1}$  less than MaxAD of B3LYP. As mentioned earlier, the X3LYP hybrid functional is a modification of B3LYP functional with the inclusion of part of exchange functional of Perdew and co-workers. Such modification has marginal effect on the final accuracy of anharmonic frequencies with VCCM.

The inclusion of Grimme's dispersion correction term to the B3LYP method reduces the accuracy of the anharmonic frequencies with VCCM method. The SD of B3LYPD (29  $\text{cm}^{-1}$ ) is about 3  $\text{cm}^{-1}$  higher than SD of B3LYP. The MaxAD of the B3LYPD is about 6  $\text{cm}^{-1}$  higher than MaxAD of the B3LYP.

The Minnesota family functionals M06 and M062x that give accurate results for thermo-chemistry, are found to perform poorly for the anharmonic frequency calculations compared to the standard hybrid functionals B3PW91, B3P86, PBE1PBE, X3LYP and B3LYP. The SD values of M06 and M062x are 33.7 and 31.8  $\text{cm}^{-1}$ , respectively, and the MaxAD values are 112 and 133  $\text{cm}^{-1}$ , respectively. Both the SD and MaxAD values of M06 and M062x are significantly higher than the SD and MaxAD values of five hybrid functionals. For example, the SD of M06 and M062x are about 12 and 10  $\text{cm}^{-1}$  higher than SD of B3PW91, respectively. Between M06 and M062x, we find that M062x gives marginally better results than M06 in terms of the SD values. However, the MaxAD of M06 is about 20  $\text{cm}^{-1}$  less than MaxAD of the M062x.

Our results suggest that the long-range corrected LC- $\omega$  PBE is significantly less accurate than the standard hybrid functionals and Minnesota functionals for VCCM frequencies. The SD of LC- $\omega$ PBE (41.4  $\text{cm}^{-1}$ ) is almost twice of SD of B3PW91, and about 1.5 times of B3LYP. Again, the MaxAD value of LC- $\omega$ PBE (162  $\text{cm}^{-1}$ ) is almost double of MaxAD value of B3PW91, and about 45  $\text{cm}^{-1}$  higher than MaxAD value of B3LYP calculations. Compared to Minnesota functionals, e.g., M062x, the SD value of LC- $\omega$  PBE is about 10  $\text{cm}^{-1}$  higher. Similar pattern is also found in the MaxAD values.

Among all the functionals studied here, the pure functional BLYP is found to be the most inaccurate method for anharmonic frequencies. The SD value of BLYP is as high as 79.9  $\text{cm}^{-1}$ , and the MaxAD value is 267  $\text{cm}^{-1}$ . This SD is about three times less than its hybrid counterpart B3LYP. Again, the MaxAD of BLYP is almost double of B3LYP. Thus, the inclusion of HF exchange improves the accuracy of the PES significantly.

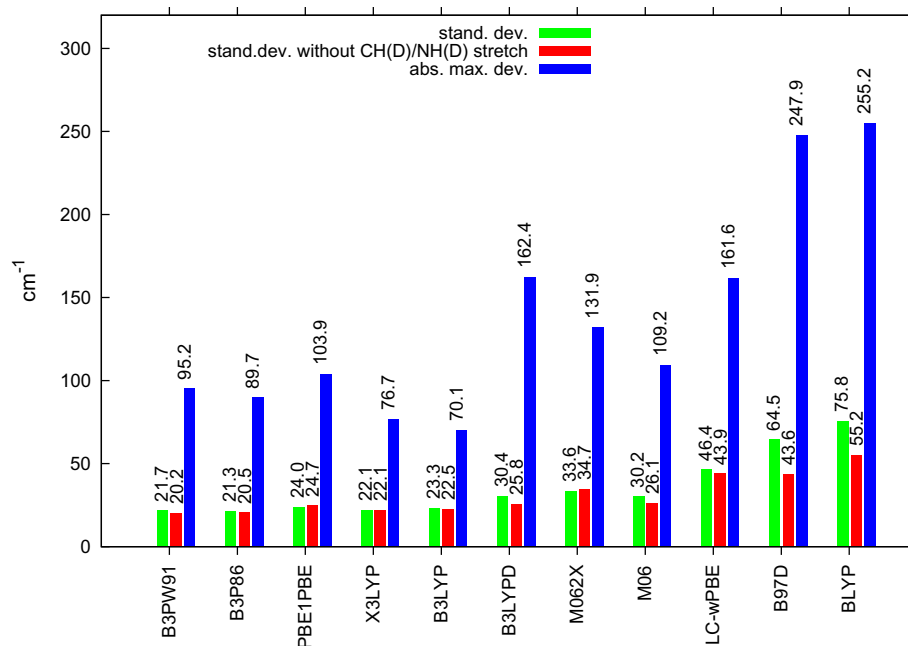
We observed large error in the VCCM frequencies with B97D functional. The SD and MaxAD values with B97D functional are 70.7 and 228  $\text{cm}^{-1}$ , respectively. Like BLYP, the HF exchange term is absent in the B97D functional. Thus, such large errors highlight the importance of HF exchange term in the DFT functional for the accurate description of anharmonicities of polyatomic molecules. Moreover, the presence of dispersion correction in the functional may attribute to the errors in the B97D calculations, as we noticed the deterioration of accuracy with B3LYPD over B3LYP.

The deviations between the VCCM and experimental frequencies are more for high frequency CH(D) and NH(D) fundamentals for the most of the functionals. We noticed that the most of the MaxAD values are from CH(D) or NH(D) stretching fundamentals. (In Table S1 of the supplementary materials, the MaxAD value and the corresponding vibrational mode and molecule is given). As a consequence, we find a significant reduction of SD values if we exclude these high-energy modes from the SD calculations. For example, the SD value with BLYP calculation is as high as 79.9  $\text{cm}^{-1}$ , when all the modes are involved in the calculation. This error reduces to 58.9  $\text{cm}^{-1}$  if the calculation excludes the CH(D) and NH(D) stretching frequencies. However, we notice exceptions with the PBE1PBE, M062x and LC- $\omega$ PBE functionals. The SD with and without CH(D) and NH(D) stretching frequencies with these three functionals are nearly identical. These functionals give comparatively more accurate results for CH(D) and NH(D) fundamentals than others. The MaxAD values are from the N-N stretching mode of *trans*-N<sub>2</sub>D<sub>2</sub> molecule for these three methods.

In Fig. 2, we present the SD and MaxAD values of VPT2 calculations. We find that the patterns of the VCCM and VPT2 results are very similar. The standard hybrid functional B3LYP, B3P86, B3PW91, PBE1PBE, and X3LYP give more accurate results than other functionals. These five functionals show similar accuracy for VPT2 frequencies. The differences of the SD values of error with these five functionals lie within 3  $\text{cm}^{-1}$  and their MaxAD values differ by at most 30  $\text{cm}^{-1}$ . However, unlike VCCM, we do not find any systematic improvement of final accuracy with Perdew's correlation functional over LYP correlation functional.

The inclusion of Grimme's dispersion correction to the B3LYP functional reduces the accuracy of the VPT2 results also. The SD of B3LYP, 23.3, increases to 30.4  $\text{cm}^{-1}$  with

**Fig. 2** The standard deviations of errors (in  $\text{cm}^{-1}$ ) in the VPT2 calculations



B3LYPD method. The MaxAD value of B3LYPD ( $162 \text{ cm}^{-1}$ ) is significantly higher than the MaxAD value of B3LYP ( $70 \text{ cm}^{-1}$ ).

With the VPT2 method also, the pure functional BLYP, B97D and long-range corrected LC- $\omega$ PBE give poor results. The maximum errors are found with BLYP followed by B97D. The magnitudes of errors with these three functionals are significantly higher than the errors with other functionals. For example, the SD of BLYP, B97D and LC- $\omega$ PBE are as high as  $75.8$ ,  $64.5$  and  $46.4 \text{ cm}^{-1}$ , respectively, compared to the SD of B3P86 ( $21.7 \text{ cm}^{-1}$ ).

The Minnesota functionals M06 and M062x are found to be significantly less accurate than the standard hybrid functionals in the VPT2 calculations. This trend is consistent with the VCCM results. However, unlike in VCCM, where M062x is found to be marginally more accurate than M06 method, here M06 gives better results than M062x. The SD of the M06 results is  $30.2 \text{ cm}^{-1}$ , whereas it is  $33.6 \text{ cm}^{-1}$  with M062x in the VPT2 calculations. Although the M062x functional has double amount of HF exchange compared to the M06 functional, we do not find any correlation between the amount of HF exchange terms and the accuracy of anharmonic frequencies for this class of functionals.

Next, we discuss the performance of the functionals for the individual molecules. In Tables 1 and 2, we present the SD and MaxAD from the VCCM calculations for all the molecules of our study. The good performance of the standard hybrid functionals, B3LYP, B3P86, B3PW91, X3LYP, and PBE1PBE are consistent in all the molecules. The SD as well as MaxAD values of these hybrid functionals are significantly smaller than the other functionals for almost all the molecules. These numbers are nearly equal for B3P86,

B3PW91, and PBE1PBE calculations. For example, the SD values for  $1,1\text{-C}_2\text{H}_2\text{F}_2$  molecule are  $17.9$ ,  $19.3$  and  $17.6 \text{ cm}^{-1}$ , respectively, with B3P86, B3PW91, and PBE1PBE methods, and the MaxAD values are about  $29$ ,  $31$  and  $28 \text{ cm}^{-1}$ , respectively. This pattern is reflected in the overall accuracy of these methods, as noted in Fig. 1.

We have seen in Fig. 1 that the overall accuracy of B3LYP method is less than these three functionals with Perdew's correlations. For the individual molecules also, such pattern is noticeable in the VCCM calculations. For the most of the molecules, the SD as well as MaxAD values are higher in B3LYP compared to B3P86, B3PW91, and PBE1PBE. For example, the SD of  $\text{CD}_2\text{Cl}_2$  molecule with B3LYP functional is about  $24.4 \text{ cm}^{-1}$ , whereas they are  $12.1$ ,  $12.3$ , and  $9.3 \text{ cm}^{-1}$  with B3P86, B3PW91, and PBE1PBE functionals, respectively. The MaxAD for this molecule is about  $50 \text{ cm}^{-1}$  in the B3LYP calculations and  $20$ ,  $22$ , and  $19 \text{ cm}^{-1}$  in the B3P86, B3PW91, and PBE1PBE calculations, respectively. Thus, the results of the individual molecules also suggest the better performance of Perdew's correlation functionals over LYP correlation functional. Notably, the marginal improvement of accuracy with X3LYP method over B3LYP is also consistent for almost all the molecules studied here. In the same example of  $\text{CD}_2\text{Cl}_2$  molecule, the SD and MaxAD values in the X3LYP are  $21.7$  and  $46 \text{ cm}^{-1}$ , respectively, less than B3LYP.

We noticed that the inclusion of dispersion correction to the B3LYP method reduces the overall accuracy of the anharmonic vibrations. The results in Tables 1, 2 show that such effect is consistent in all the individual molecules. Both the SD and MaxAD values for B3LYPD are systematically higher than B3LYP. However, the

**Table 1** The standard deviations in fundamental frequencies (in  $\text{cm}^{-1}$ ) by VCCM method with respect to the experimental values for each molecule of the studied set

Molecule	B3LYP	B3LYPD	B3P86	B3PW91	BLYP	B97D	M06	M062x	LC- $\omega$ PBE	PBE1PBE	X3LYP
11-C <sub>2</sub> H <sub>2</sub> F <sub>2</sub>	22.07	22.48	17.91	19.30	76.68	67.73	29.23	25.18	29.68	17.57	19.21
C <sub>2</sub> D <sub>4</sub>	16.51	18.69	14.82	14.55	57.62	50.59	23.58	24.72	40.81	17.10	16.17
C <sub>2</sub> D <sub>4</sub> O	14.67	25.98	9.77	10.92	66.91	59.29	29.02	27.16	39.25	15.18	11.73
C <sub>2</sub> H <sub>4</sub>	26.52	30.03	22.64	25.11	82.14	73.88	38.81	21.74	33.70	20.79	24.03
C <sub>2</sub> H <sub>4</sub> O	47.20	52.22	35.17	37.67	109.96	98.96	50.29	32.03	41.18	27.41	44.11
CD <sub>2</sub> Cl <sub>2</sub>	24.39	27.66	12.12	12.26	64.01	61.63	21.47	16.29	34.89	9.25	21.66
CH <sub>2</sub> Cl <sub>2</sub>	34.87	37.73	26.70	26.89	80.02	74.92	38.22	28.57	44.50	24.96	30.51
<i>cis</i> -C <sub>2</sub> D <sub>2</sub> F <sub>2</sub>	17.90	19.87	14.08	14.15	64.80	54.78	18.85	24.78	31.69	17.33	16.05
<i>cis</i> -C <sub>2</sub> H <sub>2</sub> F <sub>2</sub>	24.91	25.92	18.91	20.08	84.61	73.91	45.02	39.37	32.39	17.89	21.91
Cl <sub>2</sub> CO	26.31	27.89	22.57	21.64	64.27	52.39	36.60	40.43	52.58	29.67	25.06
D <sub>2</sub> CO	23.17	24.88	27.34	27.34	72.03	91.60	41.76	46.43	48.33	31.71	23.11
D <sub>2</sub> CS	8.34	11.10	10.53	9.67	49.21	40.46	14.55	29.28	50.44	15.70	8.98
F <sub>2</sub> CO	33.55	35.07	20.52	22.15	100.93	74.80	33.25	37.28	30.58	21.50	29.12
F <sub>2</sub> CS	28.03	30.33	10.69	12.79	90.93	66.47	13.28	23.94	30.45	13.51	23.42
Furan	20.09	28.58	24.60	15.01	77.67	61.53	36.18	18.47	29.34	20.79	26.97
H <sub>2</sub> CO	25.72	26.40	29.08	29.60	140.97	129.38	48.53	55.28	56.65	33.66	24.69
H <sub>2</sub> CS	10.67	18.43	13.90	14.72	78.10	93.29	32.79	32.82	57.85	18.30	8.94
<i>trans</i> -N <sub>2</sub> D <sub>2</sub>	32.95	32.95	40.10	39.31	90.68	71.94	46.21	64.67	84.77	49.14	33.94
<i>trans</i> -N <sub>2</sub> H <sub>2</sub>	47.38	47.96	45.31	45.82	133.96	109.75	41.60	66.24	88.31	48.72	45.09

**Table 2** The maximum deviations in fundamental frequencies (in  $\text{cm}^{-1}$ ) by VCCM method with respect to the experimental values for each molecule of the studied set

Molecule	B3LYP	B3LYPD	B3P86	B3PW91	BLYP	B97D	M06	M062x	LC- $\omega$ PBE	PBE1PBE	X3LYP
11-C <sub>2</sub> H <sub>2</sub> F <sub>2</sub>	48.80	49.67	29.37	30.62	125.72	113.94	58.76	48.32	56.96	28.33	42.52
C <sub>2</sub> D <sub>4</sub>	27.65	34.46	36.18	32.55	90.37	81.46	43.42	55.17	79.06	42.24	29.39
C <sub>2</sub> D <sub>4</sub> O	30.06	58.92	17.17	20.46	100.24	108.60	59.58	66.19	83.85	34.83	25.85
C <sub>2</sub> H <sub>4</sub>	59.25	67.15	41.59	48.10	146.67	134.16	65.04	60.76	82.54	44.99	54.15
C <sub>2</sub> H <sub>4</sub> O	118.33	124.17	75.64	79.68	203.68	194.72	108.97	72.08	90.01	67.63	113.81
CD <sub>2</sub> Cl <sub>2</sub>	50.22	58.88	20.40	22.26	108.20	105.16	32.81	33.64	47.11	19.30	45.73
CH <sub>2</sub> Cl <sub>2</sub>	61.89	70.16	55.99	57.44	125.82	121.34	83.93	57.26	84.39	52.97	57.02
<i>cis</i> -C <sub>2</sub> D <sub>2</sub> F <sub>2</sub>	38.02	40.25	24.22	24.26	99.94	84.74	40.68	53.04	67.20	32.13	33.05
<i>cis</i> -C <sub>2</sub> H <sub>2</sub> F <sub>2</sub>	54.84	58.13	42.68	46.94	134.04	128.16	111.70	72.87	75.29	31.28	49.33
Cl <sub>2</sub> CO	47.89	51.15	43.28	39.87	110.59	96.32	74.29	84.82	89.99	60.34	41.55
D <sub>2</sub> CO	37.15	36.13	56.10	52.90	101.80	177.44	74.83	88.96	90.61	68.14	42.63
D <sub>2</sub> CS	13.08	15.43	14.12	12.85	78.45	70.60	23.80	38.12	66.13	21.22	15.07
F <sub>2</sub> CO	67.30	69.40	33.93	40.90	167.35	128.76	65.00	73.31	63.95	42.82	58.93
F <sub>2</sub> CS	48.04	51.17	14.20	19.79	150.55	111.00	21.36	32.04	36.31	20.73	39.37
Furan	53.68	86.71	85.47	40.63	143.48	97.57	86.13	39.01	66.08	70.39	88.50
H <sub>2</sub> CO	37.67	36.99	60.07	56.53	267.19	255.84	89.13	96.84	98.99	73.93	43.74
H <sub>2</sub> CS	16.44	36.94	27.00	24.61	112.27	162.80	44.35	48.87	83.29	36.96	11.03
<i>trans</i> -N <sub>2</sub> D <sub>2</sub>	54.75	54.06	83.17	80.00	157.39	133.67	82.19	132.56	162.29	104.65	62.87
<i>trans</i> -N <sub>2</sub> H <sub>2</sub>	100.52	102.51	80.46	85.27	243.98	210.73	59.01	96.09	127.15	73.19	91.82

differences are not very large. This is expected since there is no weak intermolecular interaction in our systems of interest, the effect of dispersion should not be significant.

It was noted earlier by Kozuch and Martin [88] that the second derivatives of the dispersion corrections are neglected in the frequencies calculations in Gaussian09.



Thus the differences between the B3LYP and B3LYPD frequencies may be due to the anomalous behavior of the derivatives of the damping functions [88].

The results in Tables 1 and 2 suggest that the overall poor performance of the pure functionals BLYP, B97D, and long-range corrected functional LC- $\omega$ PBE are the reflection of large errors for the individual molecules. Both the SD and MaxAD values for these three functionals are much higher than the other functionals. For example, the SD for D<sub>2</sub>CS molecule in BLYP calculations (49.2 cm<sup>-1</sup>) is almost six times of SD in B3LYP (8.3 cm<sup>-1</sup>) calculations. The SD for B97D and LC- $\omega$ PBE are 40.6 and 50.4 cm<sup>-1</sup>, respectively.

Although the overall SD value with M062x is less than the SD value with M06 functional in the VCCM calculations, the results are quite scattered for the individual molecules. In about half of the molecules, the SD values are less for M06 compared to M062x. The magnitude of differences of SD values between these two methods are quite significant for some molecules. Similar pattern is found for the MaxAD values. For example, the SD of C<sub>2</sub>H<sub>4</sub>O of M06 (50.3 cm<sup>-1</sup>) is almost 18 cm<sup>-1</sup> more than the SD of M062x (32.0 cm<sup>-1</sup>). On the other hand, for *trans*-N<sub>2</sub>H<sub>2</sub> molecule, the SD of M06 (41.6 cm<sup>-1</sup>) is about 25 cm<sup>-1</sup> less than SD of M062x (66.2 cm<sup>-1</sup>). Such pattern of results makes it difficult to judge which method is more accurate over the other. It is also noted earlier that the overall accuracies with these two functionals are contradictory in VPT2 and VCCM calculations.

We present the SD values of the individual molecules with VPT2 calculations in Table 3. The MaxAD values from all the VPT2 calculations are given in the supporting information (S2). The accuracy patterns of these DFT functionals with VPT2 method are very similar to the VCCM results for the individual molecules also. The hybrid functionals B3P86, B3PW91, B3LYP, X3LYP, and PBE1PBE give more accurate results than other types of functionals. The differences of SD as well as MaxAD values among B3P86, B3PW91, and PBE1PBE functionals are very small for the individual molecules in the VPT2 results. This reflects the close behavior of these three functionals with Perdew's correlation terms for the anharmonic frequency calculations. Like VCCM calculations, the X3LYP functional improves the accuracy over B3LYP marginally for almost all the molecules. The dispersion corrected B3LYPD results are systematically less accurate than B3LYP for all the molecules with VPT2 calculations.

The VPT2 frequencies with pure functionals BLYP, B97D, and long-range corrected LC- $\omega$ PBE are the most inaccurate among the functionals for all the individual molecules. The SD values in these three functionals are significantly higher than the SD values with the other functionals, consistent with the VCCM results. Thus, we may say that the large errors with these functionals are not the artifacts of the vibrational methods used or cancelations of errors among the different molecules, they are rather due to limitations of PES generated by these three functionals.

**Table 3** The standard deviations in fundamental frequencies (in cm<sup>-1</sup>) by VPT2 method with respect to the experimental values for each molecule of the studied set

Molecule	B3LYP	B3LYPD	B3P86	B3PW91	BLYP	B97D	M06	M062x	LC- $\omega$ PBE	PBE1PBE	X3LYP
11-C <sub>2</sub> H <sub>2</sub> F <sub>2</sub>	20.04	20.82	14.15	15.01	69.76	51.62	20.57	27.05	34.26	16.12	17.64
C <sub>2</sub> D <sub>4</sub>	15.37	16.55	16.04	14.54	51.82	45.10	17.67	28.83	44.89	19.47	16.10
C <sub>2</sub> D <sub>4</sub> O	12.57	67.99	9.43	9.40	65.41	53.62	28.13	30.56	41.40	15.32	10.71
C <sub>2</sub> H <sub>4</sub>	23.51	23.87	17.79	18.27	68.96	60.62	27.10	25.50	42.77	19.35	22.54
C <sub>2</sub> H <sub>4</sub> O	29.94	53.42	21.15	23.25	85.93	73.65	42.26	34.31	51.11	24.56	28.77
CD <sub>2</sub> Cl <sub>2</sub>	23.77	27.31	11.67	11.59	63.00	60.81	19.89	17.85	35.88	9.30	21.71
CH <sub>2</sub> Cl <sub>2</sub>	30.63	34.20	23.99	23.76	76.57	72.90	34.09	28.62	44.69	22.26	28.86
<i>cis</i> -C <sub>2</sub> D <sub>2</sub> F <sub>2</sub>	19.59	21.37	15.57	15.07	63.48	53.67	19.30	26.61	32.81	18.50	17.20
<i>cis</i> -C <sub>2</sub> H <sub>2</sub> F <sub>2</sub>	20.13	21.37	33.76	36.98	78.88	67.65	43.42	33.36	30.65	31.94	18.36
Cl <sub>2</sub> CO	26.89	28.48	23.20	22.29	64.45	52.80	37.24	41.14	66.50	29.79	25.69
D <sub>2</sub> CO	24.06	26.07	27.68	27.80	97.79	90.65	42.36	45.84	47.70	31.91	24.04
D <sub>2</sub> CS	13.30	15.97	14.47	13.91	49.15	41.68	17.04	31.58	54.07	18.92	13.99
F <sub>2</sub> CO	37.40	35.81	22.97	22.94	101.78	75.57	36.14	36.87	34.40	26.47	29.88
F <sub>2</sub> CS	29.28	31.64	11.37	13.54	91.90	67.52	13.42	23.58	30.23	13.54	24.78
Furan	9.72	13.59	7.71	6.02	64.22	54.28	15.50	22.17	42.19	13.62	7.85
H <sub>2</sub> CO	29.33	77.67	31.41	32.26	136.80	127.96	52.31	51.05	53.11	35.47	28.43
H <sub>2</sub> CS	33.06	37.10	33.79	34.78	86.27	75.37	24.20	40.71	76.87	36.11	32.11
<i>trans</i> -N <sub>2</sub> D <sub>2</sub>	35.69	35.64	42.08	41.38	92.08	73.84	49.95	66.31	82.83	50.65	36.55
<i>trans</i> -N <sub>2</sub> H <sub>2</sub>	47.63	47.51	47.93	47.93	142.98	115.88	54.88	78.29	99.02	53.94	46.98

We note that the irregular behavior of SD and MaxAD values of M062x and M06 functionals for the individual molecules for the VPT2 method also. The SD and MaxAD of M06 is less than M062x for some molecules, and otherwise for the rests.

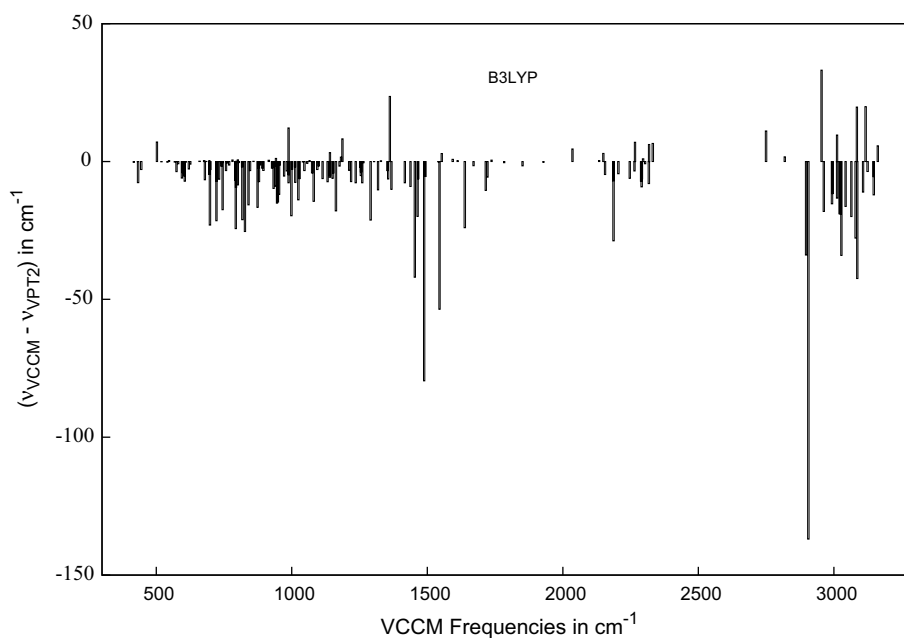
The performance of the DFT functionals under study follows similar pattern in both VCCM and VPT2 calculations. We present the plot of  $(\nu^{\text{VCCM}} - \nu^{\text{VPT2}})$  values against the VCCM frequencies in Fig. 3 for the B3LYP PES. We find that the VPT2 frequencies in our study are higher than the VCCM frequencies for the most of the fundamental transitions. These pattern is consistent for the all DFT functionals used here. (The plots of  $\nu^{\text{VCCM}} - \nu^{\text{VPT2}}$  values against the VCCM frequencies for the rest of the PESs are given in Figure S1 and S2 of Supplementary Materials). As mentioned before, the VCCM method due to its exponential parametrization of the ground-state wave function, accounts the correlation effects in a very accurate manner. In terms of perturbative analysis, it can be shown that the coupled cluster method sums up all the connected diagrams up to infinite order for a given approximation in the cluster operator [89]. Thus, the VCCM treats anharmonic effect more accurately than the VPT2. We find that differences between VCCM and VPT2 results are more prominent for the C–Cl and C–F stretching fundamentals (frequency range 1500–2000  $\text{cm}^{-1}$ ) and the high-energy C–H or N–H fundamentals (frequency range 2700–3400  $\text{cm}^{-1}$ ). These modes are highly anharmonic and strongly affected by Fermi and several higher-order resonance effects. For example, the CH and NH stretching fundamental states are usually strongly coupled with several higher quanta excited states. In the VPT2 calculations, the effects of Fermi resonances are estimated by a variational

calculation with the states involving the Fermi coupling. The effects of the higher-order couplings are still missing in its description. On the other hand, in the VCCM, a vibrational configuration interaction method like diagonalization of the effective Hamiltonian is invoked to describe the excited states. Thus, it gives a better description of the vibrational resonance effects present in the molecules.

We note that the effect of the Coriolis coupling and Watson term are included in the VPT2 calculations, while they are absent in the VCCM calculations. The Coriolis coupling effects may be quite significant for the small molecules like,  $\text{H}_2\text{CO}$ . These also contribute to the differences between the VPT2 and VCCM results. A detail study on the comparison between the VCCM and VPT2 methods in terms of the Coriolis coupling, different resonance effects should bring some more physical insights about these two methods. An accurate quartic PES like CCSD(T)/CBS is required to find quantitative estimation of the differences between these two methods. However, such study is out of the scope of the presented work.

In Figure S3 of the supplementary materials, we present the standard deviations and the corresponding MaxAD of the differences between the VCCM and VPT2 frequencies for all the DFT functionals. These SD values lie in between 14 and 25  $\text{cm}^{-1}$  and the MaxAD values lie in between 70 and 220  $\text{cm}^{-1}$ . The SD of differences in the VPT2 and VCCM frequencies are highest for the B3LYPD functional and minimum for the M06 functional. We found that except for B97D and B3LYPD functionals, both the SD and MaxAD do not differ much between the DFT functionals. The dispersion corrections in the B97D and B3LYP functionals increases the differences between VCCM and VPT2 results.

**Fig. 3** The differences between the VCCM frequencies and the VPT2 frequencies for the B3LYP PES



Next, we turn our attention to analyze the source of the discrepancies of the DFT methods for the anharmonic description of the vibrational frequencies, in terms of the harmonic and anharmonic force field description by these methods. We calculate the errors in the harmonic and anharmonic frequencies with VCCM method with respect to the experimental values as follows,

$$\Delta_{\text{harm}}^{\text{Method}} = \nu_{\text{exp}} - \nu_{\text{harm}}^{\text{Method}} \quad (14a)$$

**Fig. 4** The errors in the harmonic (green lines) and anharmonic frequencies (red lines) with respect to the experimental values for B3LYP, B3LYPD and BLYP methods

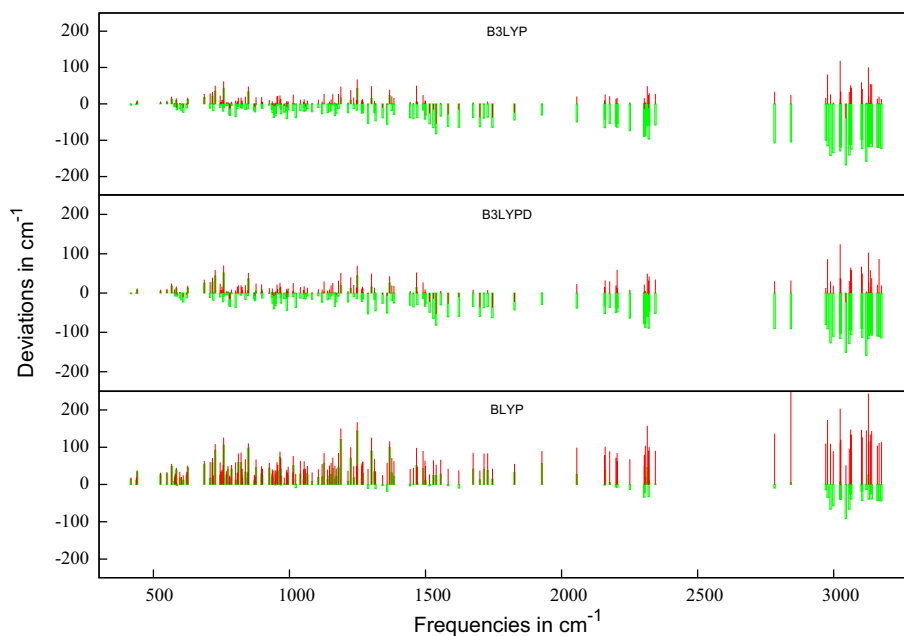
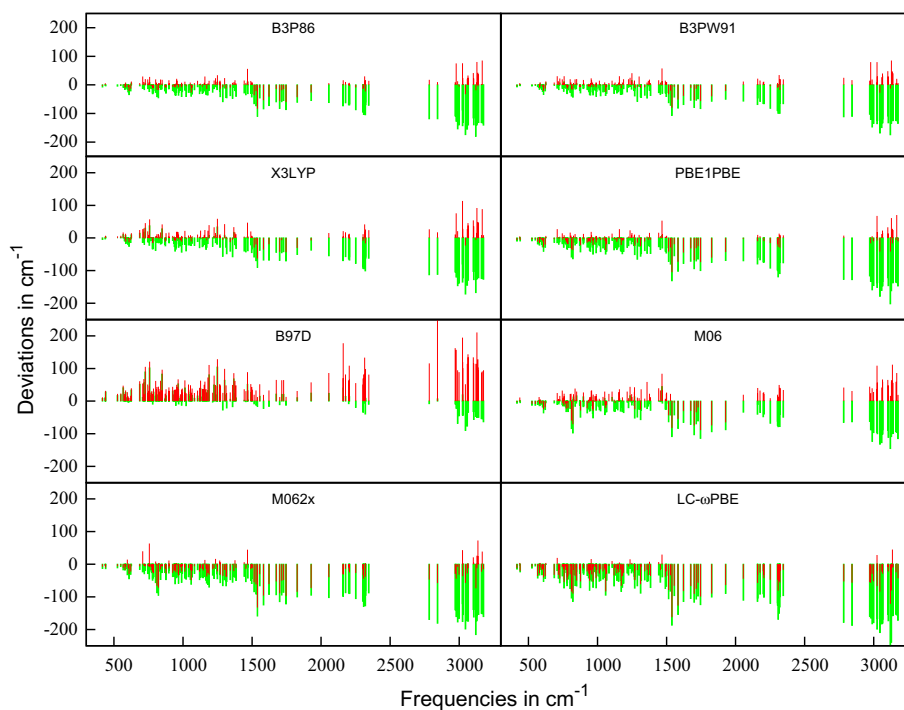


**Fig. 5** The errors in the harmonic (green lines) and anharmonic frequencies (red lines) with respect to the experimental values for different DFT functionals



$$\Delta_{\text{anh}}^{\text{Method}} = \nu_{\text{exp}} - \nu_{\text{VCCM}}^{\text{Method}} \quad (14b)$$

In Fig. 4, we present the comparison of these errors for the most widely used functional B3LYP, its dispersion corrected functional B3LYPD, and the pure functional BLYP. These three DFT methods have same type of exchange and correlation functionals. In Fig. 5, we compare the errors with other functionals.

From Fig. 4, we note that the B3LYP and B3LYPD have similar pattern for the errors  $\Delta_{\text{harm}}$  as well as  $\Delta_{\text{VCCM}}$ . The  $\Delta_{\text{harm}}$  values are negative. Except for the region 1500–2000  $\text{cm}^{-1}$ , the anharmonic corrections reduce the frequency values to a large extent and they are overestimated compared to the experimental numbers. This is more visible for the high-energy CH or NH stretching region 2700–3400  $\text{cm}^{-1}$ . The large negative  $\Delta_{\text{harm}}$  values for these modes become significantly positive after anharmonic corrections. We note that for the fundamentals in frequency region 1500–2000  $\text{cm}^{-1}$ , the  $\Delta_{\text{VCCM}}$  values are negative for these two functionals. These vibrational frequencies belong to C–F or C–Cl stretching. These two hybrid functionals underestimate the anharmonicities for these vibrational modes.

Figure 4 suggests that the large deviations of the anharmonic frequencies compared to the experimental numbers with the pure functional BLYP are due to relatively smaller values of the harmonic frequencies. Except for the CH(D) or NH(D) stretching fundamentals, the most of the harmonic frequencies are less than experimental values. Even for the CH(D) or NH(D) fundamentals, the  $\Delta_{\text{harm}}^{\text{BLYP}}$  are less negative compared to its hybrid counterpart B3LYP. The anharmonic corrections bring them down to a greater extent. Thus, we get large positive numbers for  $\Delta_{\text{VCCM}}^{\text{BLYP}}$ . The same pattern is found for the B97D functional. From Fig. 5, we find that the large errors for the VCCM frequencies with B97D functional is due to the overestimation of the harmonic frequencies compared to the experimental values.

From Fig. 5, we find that the errors in the harmonic and anharmonic frequencies with the hybrid functionals B3P86, B3PW91 and X3LYP follow similar pattern as of B3LYP results. The  $\Delta_{\text{harm}}$  are negative with these functionals. Except for the region 1500–2000  $\text{cm}^{-1}$ , the  $\Delta_{\text{VCCM}}$  values are positive due to overestimation of anharmonic effects. The anharmonic descriptions for the region 1500–2000  $\text{cm}^{-1}$  are not sufficient to counter the negative  $\Delta_{\text{VCCM}}$  values of C–F and C–Cl stretching modes with these hybrid functionals.

The overall SD and the SD for the individual molecules suggest that the accuracy of the anharmonic frequencies with PBE1PBE functional are close to B3P86 and B3PW91. However, Fig. 5 suggests that the pattern of the  $\Delta_{\text{VCCM}}^{\text{PBE1PBE}}$  values deviates from  $\Delta_{\text{VCCM}}^{\text{B3P86}}$  and  $\Delta_{\text{VCCM}}^{\text{B3PW91}}$ . For the CD or ND stretching modes (2000–2500  $\text{cm}^{-1}$ ), the  $\Delta_{\text{VCCM}}^{\text{PBE1PBE}}$  values are positive, whereas the  $\Delta_{\text{rmVCCM}}^{\text{B3P86}}$  and  $\Delta_{\text{VCCM}}^{\text{B3PW91}}$  are negative. For the frequency region 1500–2000  $\text{cm}^{-1}$ , we find larger negative errors in the anharmonic frequencies with PBE1PBE compared to B3P86 and B3PW91. For the low frequency modes in the range 300–1500  $\text{cm}^{-1}$ ,  $\Delta_{\text{VCCM}}^{\text{B3P86}}$  and  $\Delta_{\text{VCCM}}^{\text{B3PW91}}$  numbers are mostly positive, whereas,  $\Delta_{\text{VCCM}}^{\text{PBE1PBE}}$  numbers are distributed over both sides of the zero axis. Thus, significant cancelation of errors in this region reduces the overall SD value for PBE1PBE functional. On the other hand, the

anharmonic corrections are more systematic for the hybrid functionals B3PW91 and B3P86.

We find different pattern of the harmonic and anharmonic errors between the M06 and M062x methods. The errors in the harmonic calculations are negative for both these methods. However, the absolute  $\Delta_{\text{harm}}^{\text{M06}}$  values are less than the absolute  $\Delta_{\text{harm}}^{\text{M062x}}$  values. For the low energy modes of the frequency range 300–1500  $\text{cm}^{-1}$ , the  $\Delta_{\text{VCCM}}^{\text{M06}}$  values are positive and the  $\Delta_{\text{VCCM}}^{\text{M062x}}$  values are negative. Thus, M06 overestimates and M062x underestimates the anharmonic effects for this range. For the frequency range 1500–2000  $\text{cm}^{-1}$ , both the methods underestimate the anharmonicities. Again, for the CD or ND stretching modes in the frequency range 2000–2500  $\text{cm}^{-1}$ , M06 overestimates and M062x underestimates the anharmonic effects. For the high energy range 2700–3400  $\text{cm}^{-1}$ , the  $\Delta_{\text{VCCM}}^{\text{M06}}$  values are positive, and the  $\Delta_{\text{VCCM}}^{\text{M062x}}$  values are scattered over both sides of the zero axis. Thus, the accurate description of the high-energy CH(D) or NH(D) modes with M062x method is the consequence of cancelation of errors in the anharmonic descriptions. From  $\Delta_{\text{VCCM}}^{\text{M062x}}$  and  $\Delta_{\text{harm}}^{\text{M062x}}$  values, we can say that the large SD for the overall results is due to inadequate account of anharmonic effect in the M062x PESs, that is unable to bring down the large deviations of the harmonic frequencies. On the other hand, the overestimations of anharmonicities in the M06 PESs are responsible for the corresponding large SD value.

In case of LC- $\omega$ PBE functional, the resultant inaccuracy of this functional arises from both harmonic part and anharmonic part of the PES. The most of the  $\Delta_{\text{harm}}^{\text{LC-}\omega\text{PBE}}$  values are more negative than in any functionals studied here. The anharmonic corrections are not able to bring down these errors significantly. As a result, we get large SD values for the individual molecules as well as for the overall standard deviation calculation.

## 4 Summary

In this work we analyze the performance of several commonly used density functionals to generate the quartic PES for the VCCM calculations. To this end, we compute the anharmonic frequencies for the fundamental transitions of nineteen molecules. The comparative study on these DFT methods is performed in terms of the standard deviations and the maximum absolute deviations of the resultant anharmonic fundamental frequencies with respect to the experimental values. The important observations from this work can be summarized as

1. The hybrid functionals B3P86, B3PW91, PBE1PBE, B3LYP, and X3LYP give more accurate results than the other functionals studied here.

- The correlation functionals of Perdew and co-workers perform marginally better than the Lee–Yang–Parr correlation functional for the hybrid DFT method if the VCCM is used to calculate the fundamental frequencies. However, no such trend is found in the VPT2 results.
- The hybrid functionals give far better description than the standalone functionals BLYP and B97D. The HF exchange term in the hybrid density functionals improves the accuracy of the quartic PES significantly. The harmonic frequencies with B97D and BLYP functionals are significantly smaller compared to the harmonic frequencies with other functionals. The harmonic frequencies of B97D and BLYP are in fact close to the experimental values, and consequently, we get large error in the anharmonic frequencies with VCCM.
- Grimme's dispersion correction to the hybrid functional B3LYP reduces the accuracy of the results. The B3LYPD results are systematically less accurate than the B3LYP results for all the molecules studied here.
- The Minnesota functionals M06 and M062x, which give accurate results for thermo-chemistry, are found to be less accurate for anharmonic vibrations. There is no systematic trend found between the results with these two functionals. The M062x gives more accurate results than M06 for VCCM calculations, whereas for the VPT2 calculations, the M06 is more accurate. The SD values of the individual molecules also do not follow any trend in both VCCM and VPT2 calculations. Although the M062x is a modification of M06 with the double amount of HF exchange term, it does not lead to systematic improvement or deterioration of accuracy over M06.
- The long-range corrected functional LC- $\omega$ PBE accounts poor description of the anharmonic frequencies. The harmonic frequencies with this functional are higher than the harmonic frequencies with other functionals. The anharmonicities in the resultant PESs are not adequate to compensate the large error in the harmonic calculations.

## 5 Supporting information

The maximum absolute deviations for each method and the corresponding vibrational modes are given in Table S1. The maximum absolute deviations of the individual molecules with respect to the experimental values in the VPT2 calculations are given in Table S2. The VCCM frequencies for the fundamental transitions are compared with the experimental values for all the molecules in the study (Table S3 to Table S21). In Figure S1 and S2, the differences between the VCCM and VPT2 frequencies are plotted against the VCCM frequencies. Figure S3 contains the standard deviations and

maximum absolute deviations of the differences of VCCM and VPT2 frequencies.

**Acknowledgements** Lalitha Ravichandran acknowledges financial support from UGC, India, under Dr. D. S. Kothari postdoctoral fellowship scheme.

## References

- Lasch P, Kneipp J (2008) Biomedical vibrational spectroscopy. Wiley, Hoboken
- Siebert F, Hildebrandt P (2008) Vibrational spectroscopy in life science. Tutorials in biophysics. Wiley, Hoboken
- Larkin P (2011) Infrared and raman spectroscopy: principles and spectral interpretation. Elsevier, Amsterdam
- Searles D, Nagy-Felsobuki E (2013) Ab initio variational calculations of molecular vibrational-rotational spectra. Lecture notes in chemistry. Springer, Berlin
- Atkinson G (2012) Time-resolved vibrational spectroscopy. Elsevier Science, Amsterdam
- Wilson E, Decius J, Cross P (1955) Molecular vibrations: the theory of infrared and raman vibrational spectra. Dover books on chemistry series. Dover Publications, Mineola
- Frisch MJ, Trucks GW, Schlegel HB, Scuseria GE, Robb MA, Cheeseman JR, Scalmani G, Barone V, Mennucci B, Petersson GA, Nakatsuji H, Caricato M, Li X, Hratchian HP, Izmaylov AF, Bloino J, Zheng G, Sonnenberg JL, Hada M, Ehara M, Toyota K, Fukuda R, Hasegawa J, Ishida M, Nakajima T, Honda Y, Kitao O, Nakai H, Vreven T, Montgomery Jr. JA, Peralta JE, Ogliaro F, Bearpark M, Heyd JJ, Brothers E, Kudin KN, Staroverov VN, Kobayashi R, Normand J, Raghavachari K, Rendell A, Burant JC, Iyengar SS, Tomasi J, Cossi M, Rega N, Millam JM, Klene M, Knox JE, Cross JB, Bakken V, Adamo C, Jaramillo J, Gomperts R, Stratmann RE, Yazyev O, Austin AJ, Cammi R, Pomelli C, Ochterski JW, Martin RL, Morokuma K, Zakrzewski VG, Voth GA, Salvador P, Dannenberg JJ, Dapprich S, Daniels AD, Farkas o, Foresman JB, Ortiz JV, Cioslowski J, Fox DJ (2009) Gaussian09 Revision B.01. Gaussian Inc, Wallingford
- Werner HJ, Knowles PJ, Knizia G, Manby FR, Schütz M, Celani P, Gyröffy W, Kats D, Korona T, Lindh R, Mitrushenkov A, Rauhut G, Shamasundar KR, Adler TB, Amos RD, Bernhardtsson A, Berning A, Cooper DL, Deegan MJO, Dobbyn AJ, Eckert F, Goll E, Hampel C, Hesselmann A, Hetzer G, Hrenar T, Jansen G, Köppl C, Liu Y, Lloyd AW, Mata RA, May AJ, McNicholas SJ, Meyer W, Mura ME, Nicklass A, O'Neill DP, Palmieri P, Peng D, Pflüger K, Pitzer R, Reiher M, Shiozaki T, Stoll H, Stone AJ, Tarroni R, Thorsteinsson T, Wang M (2015) Molpro, version 2015.1, a package of ab initio programs
- Gordon MS, Schmidt MW (2005) Advances in electronic structure theory: GAMESS a decade later. Elsevier, Amsterdam, pp 1167–1189
- Nielsen HH (1951) Rev Mod Phys 23:90
- Barone V (2005) J Chem Phys 122:014108
- Bloino J, Barone V (2012) J Chem Phys 136:124108
- Barone V, Biczysko M, Bloino J (2014) Phys Chem Chem Phys 16:1759
- Culot F, Liévin J (1992) Phys Scr 46:502
- Carter S, Handy NC (1986) Comput Phys Rep 5:117
- Boese AD, Martin JML (2004) J Phys Chem A 108:3085
- Bowman JM (1978) J Chem Phys 68:608
- Bowman JM (1986) Acc Chem Res 19:202
- Carney DG, Sprandel LL, Kern CW (1978) Adv Chem Phys 37:305



20. Chaban GM, Jung JO, Gerber RB (1999) *J Chem Phys* 111:1823
21. Gerber RB, Chaban GM, Brauer B, Miller Y (2005) In: C.E. Dykstra, G. Frenking, K. Kim, G. Suceria (eds) *Theory and applications of computational chemistry: the first forty years*, chap. 9 Elsevier, Tokyo, pp. 165–194
22. Heislbetz S, Rauhut G (2010) *J Chem Phys* 132:124102
23. Hirata S, Hermes MR (2014) *J Chem Phys* 141:184111
24. Christiansen O, Kongsted J, Paterson MJ, Luis JM (2006) *J Chem Phys* 125:214309
25. Seidler P, Hansen MB, Györfy W, Toffoli D, Christiansen O (2010) *J Chem Phys* 132:164105
26. Neff M, Rauhut G (2009) *J Chem Phys* 131:124129
27. Seidler P, Kongsted J, Christiansen O (2007) *J Phys Chem A* 111:11205
28. Christiansen O (2004) *J Chem Phys* 120:2149
29. Seidler P, Christiansen O (2007) *J Chem Phys* 126:204101
30. Seidler P, Hansen MB, Christiansen O (2008) *J Chem Phys* 128:154113
31. Seidler P, Christiansen O (2009) *J Chem Phys* 131:234109
32. Nagalakshmi V, Lakshminarayana V, Sumithra G, Durga Prasad M (1994) *Chem Phys Lett* 217:279
33. Banik S, Pal S, Durga Prasad M (2008) *J Chem Phys* 129:134111
34. Banik S, Pal S, Durga Prasad M (2012) *J Chem Phys* 137:114108
35. Banik S, Durga Prasad M (2012) *Theory Chem Acc* 131:1383
36. Durga Prasad M (2000) *Indian J Chem* 39A:196
37. Faucheaux JA, Hirata S (2015) *J Chem Phys* 143:134105
38. Banik S (2016) *Theory Chem Acc* 135:203
39. Yagi K, Hirata S, Hirao K (2008) *Phys Chem Chem Phys* 10:1781
40. Yagi K, Otaki H (2014) *J Chem Phys* 140:084113
41. Banik S, Ravichandran L, Durga Prasad M (2014) *Mol Phys* <https://doi.org/10.1080/00268976.2017.1321153>
42. Chakraborty S, Banik S, Das PK (2016) *J Phys Chem A* 120:9707
43. Rauhut G, Barone V, Schwerdtfeger P (2006) *J Chem Phys* 125:54308
44. Ess DH, Houk K (2005) *J Phys Chem A* 109:9542
45. Andzelm J, Rinderspacher BC, Rawlett A, Dougherty J, Baer R, Govind N (2009) *J Chem Theory Comput* 5:2835
46. Thanthiriwatte KS, Hohenstein EG, Burns LA, Sherrill CD (2010) *J Chem Theory Comput* 7:88
47. Maroulis G (2006) *Structure and properties of clusters: from a few atoms to nanoparticles*. CRC Press, Boca Raton, p 103
48. Siegbahn PE (2006) *J Biological Inorg Chem* 11:695
49. De Proft F, Martin JML, Geerlings P (1996) *Chem Phys Lett* 250:393
50. Zhang G, Musgrave CB (2007) *J Phys Chem A* 111:1554
51. Carbonniere P, Lucca T, Pouchan C, Rega N, Barone V (2005) *J Comput Chem* 26:384
52. Barone V (2004) *J Phys Chem A* 108:4146
53. Biczysko M, Panek P, Scalmani G, Bloino J, Barone V (2010) *J Chem Theory Comput* 6:2115
54. Daniel Boese A, Klopper W, Martin JML (2005) *Mol Phys* 103:863
55. Kesharwani MK, Brauer B, Martin JML (2015) *J Phys Chem A* 119:1701
56. Becke AD (1988) *Phys Rev A* 38:3098
57. Perdew JP, Burke K, Ernzerhof M (1996) *Phys Rev Lett* 77:3865
58. Becke AD (1993) *J Chem Phys* 98:5648
59. Lee C, Yang W, Parr RG (1988) *Phys Rev B* 37:785
60. Cohen AJ, Mori-Sanchez P, Yang W (2012) *Chem Rev* 112:289
61. Zhao Y, Truhlar DG (2005) *J Chem Theory Comput* 1:415
62. Lewars E (2010) *Computational chemistry: introduction to the theory and applications of molecular and quantum mechanics*. Springer, Netherlands
63. Cheron N, Jacquemin D, Fleurat-Lessard P (2012) *Phys Chem Chem Phys* 14:7170
64. Kang JK, Musgrave CB (2001) *J Chem Phys* 115:11040
65. Song JW, Hirokawa T, Tsuneda T, Hirao K (2007) *J Chem Phys* 126(15):154105
66. Grafenstein J, Cremer D (2000) *Phys Chem Chem Phys* 2:2091
67. Pople JA, Head-Gordon M, Fox Douglas J, Raghavachari K, Curtiss LA (1989) *J Chem Phys* 90:5622
68. Vosko SH, Wilk L, Nusair M (1980) *Can J Phys* 58:1200
69. Grimme S (2006) *J Comput Chem* 27:1787
70. Perdew JP (1986) *Phys Rev B* 33:8822
71. Perdew JP (1991) In: Ziesche P, Eschrig H (eds) *Electronic structure of solids*. Akademie Verlag, Berlin, p 11
72. Adamo C, Barone V (1999) *J Chem Phys* 110:6158
73. Grimme S (2006) *J Comp Chem* 27:1787
74. Becke AD (1997) *J Chem Phys* 107:8554
75. Vydrov OA, Scuseria GE (2006) *J Chem Phys* 125:234109
76. Xu X, Goddard WA (2004) *Proc Natl Acad Sci USA* 101:2673
77. Zhao Y, Truhlar DG (2008) *Theory Chem Acc* 120:215
78. Christiansen O (2007) *Phys Chem Chem Phys* 9:2942
79. Banik S, Pal S, Durga Prasad M (2010) *J Chem Theory Comput* 6:3198
80. Roy TK, Durga Prasad M (2009) *J Chem Sci* 121:805
81. Mukherjee D (1979) *Pramana* 12:203
82. Madhavi Sastry G, Durga Prasad M (1993) *Theory Chim Acta* 89:511
83. Mukherjee D, Mukherjee P (1979) *Chem Phys* 39:325
84. Monkhorst HJ (1977) *Int J Quantum Chem* 12(S11):421
85. Dutler R, Rauk A (1989) *J Am Chem Soc* 111:6957
86. Kwiatkowski JS, Leszczynski J, Teca I (1997) *J Mol Struct* 436–437:451
87. NIST chemistry webbook, NIST standard reference database number 69, national institute of standards and technology. <http://webbook.nist.gov/chemistry/>
88. Kozuch S, Martin JML (2013) *J Comput Chem* 34:2327
89. Bartlett RJ, Musial M (2007) *Rev Mod Phys* 79:291